



Published in final edited form as:

*Macromolecules*. 2010 March 23; 43(6): 2643–2653. doi:10.1021/ma902596s.

## Covalent Adaptable Networks (CANs): A Unique Paradigm in Crosslinked Polymers

Christopher J. Kloxin<sup>†</sup>, Timothy F. Scott<sup>‡</sup>, Brian J. Adzima<sup>†</sup>, and Christopher N. Bowman<sup>\*,†</sup>

<sup>†</sup> Department of Chemical and Biological Engineering, University of Colorado, Boulder, CO 80309-0424, USA.

<sup>‡</sup> Department of Mechanical Engineering, University of Colorado, Boulder, Colorado 80309-0427, USA.

### Abstract

Polymer networks possessing reversible covalent crosslinks constitute a novel material class with the capacity for adapting to an externally applied stimulus. These covalent adaptable networks (CANs) represent a trend in polymer network fabrication towards the rational design of structural materials possessing dynamic characteristics for specialty applications. Herein, we discuss the unique attributes of CANs that must be considered when designing, fabricating, and characterizing these smart materials that respond to either thermal or photochemical stimuli. While there are many reversible reactions which to consider as possible crosslink candidates in CANs, there are very few that are readily and repeatedly reversible. Furthermore, characterization of the mechanical properties of CANs requires special consideration owing to their unique attributes. Ultimately, these attributes are what lead to the advantageous properties displayed by CANs, such as recyclability, healability, tunability, shape changes, and low polymerization stress. Throughout this perspective, we identify several trends and future directions in the emerging field of CANs that demonstrate the progress to date as well as the essential elements that are needed for further advancement.

### 1. Introduction

Polymer networks have been variously described as “branching to its extreme”<sup>1</sup> or, perhaps more precisely, as “indefinitely large polymer structures”<sup>2</sup>. Covalently crosslinked networks, or thermosets, are extensively used as structural materials in a vast array of applications ranging from coatings to composites to biomaterials. Additional chemical functionality is readily incorporated into these networks by the inclusion of the desired functional groups in monomers that are present during material fabrication; however, once set, these covalently crosslinked networks are, almost by definition, not readily amenable to any modification of their physical state or chemical structure. To address this significant shortcoming, recent synthetic strategies have incorporated reversible covalent bonds into these networks either within the crosslinks or the backbone structure to facilitate adaptability in these otherwise intractable materials. Herein, we define covalent adaptable networks (CANs) as those networks which contain a sufficient number and topology of reversible covalent bonds so as to enable the crosslinked network structure to respond chemically to an applied stimulus. This response, which is generally a change in the stress and/or shape (strain) of the material, is achieved without necessitating any irreversible degradation of the network structure, being capable of maintaining the initial bond density while allowing the material to rearrange. These CANs are

\* christopher.bowman@colorado.edu.

therefore ‘smart’ materials capable of responding to a stimulus with a change in the physical structure, state, and/or shape of the network.

While characteristics of traditional thermosets are ideal for many applications, where dimensional stability, environmental resistance, and permanence are required, the recycling, reuse, and post-polymerization manipulation of such materials is limited. The applications of CANs are those that require or benefit from the thermal, mechanical, and other properties of a network, but not the permanence of a typical thermoset. The potential for CANs as a reversible adhesive or as a crack-healing material has far reaching implication into a variety of technologies, from microelectronics<sup>3-6</sup> to non-linear optics<sup>7, 8</sup> to dental materials. Furthermore, CANs inherently have the ability to incorporate other chemical functionality post-polymerization, providing a flexible scaffold that is readily modified to incorporate new and important mechanical and chemical properties. This material design feature, which is often employed in supramolecular science, allows network adaptation toward chemical and environmental cues, yielding a dynamic response property that embodies the emerging field of ‘smart’ materials.

Since the first conclusive structural determination, polymer networks have been traditionally characterized as being either chemical or physical gels owing to their covalent bond structure or connectivity associated with physical associations, respectively. Indeed, this convenient designation has provided the framework for generalizing the physicomaterial behavior of these network types; for example, chemical gels are often characterized by their inability to be melted, molded, mended or otherwise permanently deformed. Nevertheless, this distinct classification is limited in its applicability as there are several material types, such as Diels-Alder networks, that are classically defined as a chemical gel though under certain circumstances they exhibit behavior more akin to that of physical gels, depending on the timescale of the experiment and the temperature. It is clear that material classification based on bond type, without consideration to bond dynamics, is insufficient to provide an accurate gauge of the network's mechanical behavior and characteristics. The presumed intransient chemical gel behavior is based on the presumed static nature of the linkages which constitute the network. For those chemical gels which have reversible covalent linkages due to the inclusion of bonds for which the bond structure is covalent yet exhibiting dynamic reversible chemistry, the network behavior depends, even qualitatively, on the timescale of the evaluation relative to the average timescale of the bond reversibility.

When considering the characteristics of a strong versus a weak gel, de Gennes argued that the essential difference is the stability of the crosslinks.<sup>9</sup> For strong gels, the crosslinks are stable for all relevant experimental timescales and stresses, while the crosslinks in weak gels are formed by a reversible reaction.<sup>9</sup> Implementation of reversible covalent or physical linkages into supramolecular structures constituted a class of material that Skene and Lehn termed “dynamers”;<sup>10</sup> thus, as a network forming material, dynamers are simply weak gels. CANs are uniquely classified by their potential to demonstrate weak gel adaptability via reversible covalent chemistry where the reversibility may be inherent in the nature of the crosslinks or triggered by an externally applied stimulus. For example, in the absence of irradiation, photoreversible CANs remain a strong gel while exposure to radiation transforms the material, transiently, into a weak chemical gel. Other CANS, such as thermoreversible CANS, are by definition weak chemical gels on an infinite timescale, but practically only demonstrate observable weak chemical gel characteristics at elevated temperatures. In practice, only a small group of the thermoreversible reactions truly form CANs as most of the thermal reversion processes are essentially depolymerization mechanisms that irreversibly degrade the network structure, removing the potential for the network to adapt while simultaneously retaining its topology and crosslink density.

In this perspective, we describe several areas of development in the field of CANs while also outlining their unique material properties. The chemistries used to produce networks of these types are reviewed along with the advantages and disadvantages of each approach. Particular focus is given to the relative degree to which the polymer is capable of adapting as dictated by the molecular rearrangement mechanisms that are incorporated into the network's chemical structure.

## 2. CAN structure and fabrication

Chemical reactions capable of undergoing reversible addition are the basic constituents of CANs. While there are several reversible condensation reactions that make up dynamic covalent chemistry,<sup>11</sup> the evolution and subsequent loss of a small molecular species eliminates the material's capacity to reversibly form a network. CANs are fabricated from monomers with reversible linkages (e.g., the Diels-Alder adduct shown in Figure 1, panel A) that are formed as part of the network fabrication process (e.g., Figure 1, panel B) or flanked by network forming functional groups (e.g., Figure 1, panel C). In this former process, the network formation mechanism is inherently step-growth and forms a structure having at least one reversible linkage per crosslink (e.g., the panel B inset has 2 reversible linkages per crosslink). In contrast, the network structure for the latter monomer type is entirely defined by the polymerization reaction of the flanking polymerizable functional groups. The example shown in panel C, Figure 1 consists of a Diels-Alder adduct flanked by acrylate groups that are capable of undergoing a radical-initiated, chain-growth polymerization or a base catalyzed step-growth co-polymerization with a multifunction thiol monomer. The network topology, resulting from the differing mechanisms, is vastly different where the chain-growth polymerization consists of ideally linear polymers crosslinked by DA adducts (inset *i* panel C, Figure 1) while the step-growth, copolymerization consists of monomeric-sized units each linked via a DA adduct (inset *ii*, panel C, Figure 1). The addition of chain transfer agents will decrease the contiguous polymer length not containing a reversible linkage. When this non-reversible contiguous polymer length approaches that of the monomer, the network structure approaches that of a step-growth mechanism.

### 2.1. Chemistries for Thermoreversible CANs

All bimolecular addition reactions are, to some extent, reversible as dictated by the temperature dependence of the equilibrium constant. Nevertheless, most reactions can essentially be considered irreversible as there are several temperature constraints that exclude the majority of these reactions from being a thermoreversible CAN building block, including consideration of a practical temperature range, high temperature induced side reactions, and chemical decomposition temperatures. Moreover, the forward and reverse reaction rates (i.e., the kinetics) must allow for bond rearrangement on an application appropriate timescale such that the network is able to adapt to an environmental stimulus. Therefore, both thermodynamic and kinetic elements of a given thermoreversible reaction must be taken into account while also considering the application and its timescale.

There are several thermoreversible crosslinking reactions that have been used to fabricate thermoreversible networks, such as those shown in Figure 2. Several of these reactions have been summarized in Engle and Wagner's 1993 review of thermoreversible polymers.<sup>16</sup> However, many thermoreversible reactions have practical limitations, such as limited reversibility owing to side reactions, precluding them from CANs applications. Here, we will note a few of the more recent utilizations of thermoreversible crosslinks, with a particular emphasis on reactions that proceed at practical rates without the use of a catalyst.

Nucleophilic addition reactions are well suited as thermoreversible reactions as they do not produce a condensate; however, the nucleophile must also be a good leaving group in order to

be reversible over a reasonable temperature range. For example, the reaction of an isocyanate with a nucleophile such as an alcohol or amine is thermoreversible, but inadequate for CANs applications. Whereas the reaction of isocyanate with imidazole has been successfully demonstrated as able to form a thermal CAN under inert conditions (reaction 1 in Figure 2),<sup>17</sup> the intolerance of isocyanates to moisture significantly limits its implementation. Nucleophilic addition reaction involving ring opening have also received attention as thermal CANs. Linear polymers with either pendant maleic acid<sup>23, 24</sup> or azlactone<sup>25</sup> functional groups crosslinked by a bis-alcohol have been shown as a viable thermoreversible crosslinking reaction; however, these materials have limited reversibility owing to various side reactions.<sup>26</sup> Carbene dimerization is another candidate reaction for the basis of a thermal CAN (reaction 2 in Figure 2). Thus far, this reaction has been used to fabricate linear polymers;<sup>18</sup> however, a network could be fabricated by flanked polymerizable functionalities (similar to shown in Figure 1, panel C). Nevertheless, carbenes tend to be highly reactive species and the exposure of carbene species shown in Figure 2 to oxygen results in the irreversible formation of a cyclic urea.<sup>18</sup>

The thermoreversible homolytic cleavage of the alkoxyamine bond (reaction 3 in Figure 2), producing both a stable, non-propagating radical [e.g., 2,2,6,6-tetramethylpiperidinyl-1-oxy (TEMPO)] and an active radical (e.g., a styryl radical), has been utilized extensively in nitroxide mediated living/controlled radical polymerizations as well as in the formation of CANs (see Figure 3). With respect to CAN formation, the production of the active radical often limits the reversibility of the material since it is capable of undergoing bimolecular termination. Nevertheless, this active radical has been utilized to incorporate other functionality into the network, by swelling the network with monomer, followed by heating the material.<sup>27</sup> Higaki et al.<sup>19</sup> utilized this reaction to crosslink linear polymers having pendant TEMPO and styryl radicals that were capped with the corresponding styryl and TEMPO radical species, respectively, to facilitate the initial network fabrication. Although the crosslinking reaction produces a small molecular weight species, the absence of this species does not prevent crosslink thermoreversibility. One prospect for thermoreversible homolytic cleavage-type linkages for CANs is use of a disulfide-based TEMPO analogue, such as Bis(2,2,6,6-tetramethylpiperidyl-1) disulfide (TEMPS). This compound exhibits both photo- and thermolytic cleavage, producing a stable, non-propagating sulfur radical and, in principle, would produce a CAN that does not undergo irreversible termination.<sup>28, 29</sup>

While each of these synthetic methodologies has its own unique advantages, the cyclical reversion potential of the [4+2] cycloaddition, known as the Diels-Alder (DA) reaction, DA-based gels is unmatched. This owes to the fact that the DA reaction exhibits many of the attributes of a click-type reaction<sup>30</sup> that is reasonably tolerant of typical environmental species such as water and oxygen and can be tuned to be responsive over a wide range of temperatures through changes in the reactive functionalities. The DA reaction has been used extensively to create thermoreversible polymer networks between a conjugated diene and, typically, an electronically activated double bond (i.e., a dienophile).<sup>31</sup> Several researchers have utilized the ability of cyclopentadiene to act as both a diene and dienophile, forming a crosslinking dimer.<sup>32, 33</sup> In a 1969 patent, Craven describes a material that is reshaped upon heating, but forms an insoluble network upon cooling.<sup>20</sup> This material was synthesized by the crosslinking of linear polymers having pendant furan moieties with (bis)maleimide and (tris)maleimide moieties via a DA reaction (reaction 4 in Figure 2). Several researchers have adopted this strategy;<sup>34-43</sup> however, the common use of functionalized linear chains, which essentially act as a macromonomer with a high degree of functionality, significantly reduces the gel's ability to undergo a gel-to-sol transition. Thus, other researchers have utilized low molecular weight, low functionality diene and dienophile monomers, e.g., a trifuran with a bismaleimide, to increase dramatically the gel-point conversion and significantly improve the ability of these systems to revert to liquids at reasonable temperatures.<sup>12, 44-49</sup>

Furan and maleimide have been the predominant functional groups used to create thermoreversible CANs. Their selection is attributed to the convenient temperature range in which this reaction shifts from products to reactants. Unfortunately, many networks that utilize diene and dienophile pairs require excessive heating to undergo the retro-DA reaction, which can also trigger irreversible side reactions. Despite the attention that furan-maleimide networks have received, there is still a need to characterize these novel materials. In particular, the kinetics of the forward and reverse reactions as a function of temperature (i.e., pre-exponential factor and activation energy), which determines the adaptation timescale, is largely absent from the thermoreversible network literature.

Recently there has been an emergence of interest in finding alternative diene and dienophile candidates to be used as thermoreversible linkages. Lehn and coworkers have explored diene and dienophile functional groups as dynamic covalent linkages in supramolecular chemistry (Reactions 5 & 6 in Figure 2).<sup>21, 22</sup> They extended these novel linkages in a network and observed self-healing properties.<sup>50</sup> In this regard, CANs represent the convergence of smart covalent networks with supramolecular science.

## 2.2. Chemistries for Photochemically reversible CANs

In addition to thermoreversible CANs, two distinct approaches to photochemically triggered CANs have also been developed. These processes, which utilize light to reversibly break and reform bonds, include photoinduced cyclization reactions and photochemical radical-mediated addition-fragmentation approaches. Unlike thermoreversible CANs, photoreversible networks only undergo bond rearrangement upon irradiation, otherwise exhibiting little to no creep or adaptation in the absence of irradiation. Photochemical approaches have the clear advantage of enabling the 3D spatial control of the reversion as well as the ability to remotely trigger a process on and off. The cyclization reactions are limited in their relative response rate, as at most a single crosslink is reversibly broken for each absorbed photon. Conversely, the addition-fragmentation reactions undergo a network rearrangement cascade, where multiple reversible bond breaking and reforming reactions occur for each absorbed photon. However, the addition-fragmentation reactions are limited by never having a large fraction of the bonds cleaved at a given time, thus restricting such materials from any applications where a gel-to-sol transition is required.

Photoinduced cyclization reactions, hereafter referred to as photodimerizations, occur when two functionalities incorporating carbon-carbon double bonds undergo a photoinduced cycloaddition reaction. The corresponding photoscission reaction is achieved simply by exposure of the sample to a different irradiating wavelength. This process, with its associated ability to spatially pattern material processes and network structures, has been utilized extensively for reversible polymer network connectivity rearrangement. Several functionalities, including coumarins,<sup>51-55</sup> cinnamates,<sup>56-60</sup> anthracenes,<sup>61-63</sup> and thymines<sup>64</sup> have been investigated to effect this polymer network rearrangement. With the exception of anthracenes, which undergo a [4+4] cycloaddition (Figure 4), photodimerization typically proceeds *via* a [2+2] cycloaddition of ethylenic bonds (Figure 4). Near-ultraviolet irradiation of materials incorporating photodimerizable functionalities effects the forward, cycloaddition reaction while irradiation at shorter wavelengths favors the reverse, scission reaction. Thus, these reactions are analogous to the thermally-controlled Diels-Alder forward and retro reactions where the light intensity, controlling the rates of the forward and reverse reactions and wavelength, controlling the equilibrium extent of the cyclization and scission reactions, are analogous to the temperature control that is exerted over Diels-Alder and other thermoreversible systems. In keeping with that analogy, the photoinduced cyclization systems are unique among the photochemical CANs in that, with sufficient light exposure at the

appropriate wavelength, they are capable of reverting to a liquid state with the assorted benefits of crack healing and mending available to materials in that state.

In addition to the photoinduced cycloaddition, photoinduced, radical-mediated addition-fragmentation approaches have recently been exploited in the formation of photoresponsive CANs. This technique exhibits all the advantages of photoinduced reactions whereby the network exists in a permanent, nonadaptable state in the absence of light, the network adaptation response is photopatternable, and the adaptation process can be commenced and ceased on demand. Moreover, addition-fragmentation chain transfer functional groups are readily incorporated into the backbone of monomers (and subsequently polymer networks) possessing a wide variety of polymerizable functionalities. Since this process employs a radical reaction, the opportunity exists for each absorbed photon to induce a chain process whereby each radical causes multiple reactions. This form of adaptability in crosslinked networks takes advantage of mechanisms that have traditionally been employed in small molecule chemistry. Here, radicals are known to react with allyl sulfides to effect homolytic substitution displacement of the thiyl group (i.e.,  $S_H2'$ ).<sup>65, 66</sup> The recognition that this mechanism could be utilized for chain transfer during radical polymerizations of styrene and methyl methacrylate lead to controlled molecular weight linear polymers possessing terminal vinyl groups.<sup>67, 68</sup> The same mechanism was subsequently used in radical ring-opening polymerizations whereby cyclic monomers consisting of 7- and 8-membered rings incorporating an allyl sulfide functionality underwent radical-mediated ring opening and continued propagation.<sup>69-75</sup>

A unique, photoinduced, nondestructive scission approach was recently developed for rearranging network connectivity by utilizing allyl sulfide functionalities incorporated in the backbone of crosslinked polymers.<sup>76-78</sup> These polymer networks were fabricated such that a significant residual amount of a radical generating photoinitiator remained after polymerization. Thus, upon irradiation subsequent to fabrication, cleavage of the residual photoinitiator introduces radicals into these materials, initiating the addition-fragmentation chain transfer reaction (shown in Figure 5) and ultimately effecting network adaptation. In post-polymerization studies, allyl sulfide containing networks demonstrated the utility of this phenomenon *via* photoinduced creep, stress relaxation, and photoinduced actuation. In a similar manner to the vulcanized rubbers studied by Tobolsky,<sup>79, 80</sup> irradiating these samples while a tensile stress is applied, network rearrangement due to the reversible addition-fragmentation chain transfer process allows for either stress relaxation or creep, depending on the mode of the applied stress, and the equilibrium shape and state of the material is altered (i.e., permanent set, Figure 6). Unlike its photodimerization/photoscission counterpart, this approach does not effect a concomitant variation in the crosslink density since, although individual bonds are being broken and reformed, the overall crosslink density remains essentially constant before during and after exposure. Moreover, while photodimerization/photoscission systems exhibit a photon to reaction event ratio no greater than one, where one photon at most either causes one addition or one scission event, a single photon absorbed in the addition-fragmentation chain transfer system leads to at most a single cleavage event of a photoinitiator molecule. However, following the radical formation as a result of the initiator cleavage, each radical can lead to a cascade of many chain transfer events, i.e., crosslink breakage and reformation. It should also be noted that the introduction of radicals is not limited to photoactivation; other stimuli such as heat to induce decomposition of thermal initiators, or exposure to chemical species able to induce redox reactions,<sup>81, 82</sup> are capable of effecting radical production and network adaptation.

Photoactivation of network rearrangement allows for facile definition of the region where stress relaxation occurs, whether that process is controlled by masking of the incident light to control stress relaxation effectively over the incident area of the sample or by controlling the absorption or focus of light throughout the thickness of the sample to control stress relaxation differentially

through the film thickness. For example, by irradiating optically thick samples under tension, a stress gradient is readily induced through the sample thickness with stresses rapidly relieved on the incident surface and much more slowly relieved at the bottom of the sample, i.e., the non-incident surface. Upon release from the externally applied stress, such a sample deforms by curling to equilibrate the internal stress (see Figure 7). Ultimately, such samples exhibited photoinduced actuation which was realized by subsequent irradiation of the previously unirradiated side, resulting in straightening of the sample, with the sample progressing back towards its original shape.<sup>77</sup>

### 3. Mechanical Properties and Gelation of CANs

Inherent to a polymer network is the transition from a mixture of small molecular species to a material having at least one sample-spanning molecule, which defines the incipient gel. The gel-point conversion is the precise point in the progression of a polymerization where the incipient gel is formed. In addition to providing a functional mathematical definition (i.e., where  $M_w$  diverges), it typically coincides with the experimentally observed transition of a completely soluble mixture to one having a fraction of insoluble gel (i.e., a sol-to-gel transition). To this extent, the formation and definition of a polymer network is well developed and generally accepted among the greater polymer science community. Here, we use a similar definition of the network structure while noting that for CANs, the gel point now depends on the timescale on which one evaluates the formation of a sample-spanning molecule.

The main characteristic imparting CANs with their unique material behavior owes to the capability of the crosslinks to reversibly break and reform. Since CANs are chemical networks that exhibit weak gel characteristics at appropriate timescales in thermoreversible systems, at appropriate light intensities in photocyclization systems, or at appropriate radical concentrations in photoinduced addition/fragmentation systems, the mechanical properties can be similar to those observed in physical gels, such as gelatin.<sup>84</sup> Specifically, consider for thermoreversible CANs that given enough time and under appropriate reversibility conditions, the polymer network will demonstrate plasticity or flow. As recognized by de Gennes, such behavior precludes weak gels from possessing a gel-point as traditionally defined in chemical gels by the divergence in the viscosity and the emergence of a finite zero-frequency elastic modulus (i.e., Young's modulus).<sup>9</sup> However, CANs must possess a gel point, as it is a prerequisite for network formation.

Dynamic mechanical analysis (DMA) is perhaps the best method for gel-point determination, since it allows for the direct measurement of elastic and viscous moduli and their temporal scaling. Winter and Chambon experimentally demonstrated that chemical gels exhibit similar frequency scaling at the gelpoint (i.e.,  $G' \sim G'' \sim \omega^\Delta$ ), which is now referred to as the Winter-Chambon criterion.<sup>85-88</sup> Since the incipient gel is characteristically fractal, it possesses the same ensemble averaged similarity on all but the smallest length-scales; thus, the temporal-spatial interpretation dictates that the elastic and viscous moduli should scale similarly with frequency.<sup>89, 90</sup> In practice, the Winter-Chambon criterion is not applicable to the entire frequency range. As previously alluded, the Winter-Chambon criterion fails at high-frequencies, owing to the onset of glassy dynamics. The type of the gel also effects the applicability of the Winter-Chambon criterion. For example, the gel point of a crosslinked, entangled polymer exhibits similar scaling only in the terminal region of the spectrum and the plateau and high-frequency region are relatively unaffected by the crosslinking.<sup>91</sup> Additionally, weak gels depart from the similar scaling behavior in the low-frequency, terminal region, owing to bond-breaking and -reforming.<sup>12, 92</sup> Thus, one can determine the gel-point of a CAN using the Winter-Chambon criterion provided that the timescale of bond-breaking and -reforming is sufficiently long to observe the elastic and viscous moduli scaling identically with frequency. Furthermore, the Winter-Chambon criterion must be used with caution as, although similar

scaling does occur at the gel point, self-similarity by itself does not necessitate the existence of a gel.

Remarkably, the DMA of most thermoreversible CANS near the gel-point temperature have not been rigorously examined. DMA measurements are available for several systems,<sup>40, 42, 93, 94</sup> but are performed at a finite rate that may not allow the system to obtain thermodynamic equilibrium. Additionally, these experiments are often limited to single frequency scans, which only reveal the crossover of the storage and loss moduli rather than establishing the gel point by the Winter-Chambon criteria. Networks formed by the DA reaction between a trifunctional furan and a difunctional maleimide (structures shown in Figure 1, panel C) were recently examined,<sup>12</sup> which have a Flory-Stockmayer predicted gel-point conversion of 0.71 and yield a gel-point temperature of  $92.5 \pm 0.5^\circ\text{C}$  as determined using FTIR spectroscopy. Figure 8 shows the complex stress relaxation moduli for three frequency sweeps above ( $95^\circ\text{C}$ ), near ( $91^\circ\text{C}$ ), and below ( $87^\circ\text{C}$ ) the gel-point temperature. The material near the gel-point exhibits the Winter-Chambon expected similar scaling at higher frequencies, while demonstrating the terminal relaxation scaling of a viscoelastic liquid at lower frequencies (i.e.,  $G' \sim \omega^2$  and  $G'' \sim \omega^1$ ) due to bond rearrangement at longer timescales.

At elevated temperatures the material exists as a liquid, with a loss modulus that is greater than the storage modulus (triangles in Figure 8). As the network is cooled below the gel-point temperature, the crosslinking increases and the elastic modulus dominates the viscous modulus for intermediate timescales (squares in Figure 8). The bond rearrangement rate of the networks slows as indicated by a terminal relaxation shift to lower frequencies. Further cooling shifts the crossover point to longer and longer times until it can no longer be observed with DMA ( $\sim 10^{-2}$  rad/s).

In the absence of kinetic limitations, such as vitrification<sup>12</sup> or crystallization<sup>95</sup>, bond formation in thermoreversible CANS is dictated by thermodynamic equilibrium and thus the equilibrium functional group conversion is dictated by the temperature. Uniquely in these thermoreversible CANS, the equilibrium constant,  $K$ , provides a direct relationship between the gel-point temperature and the gel-point conversion (see Figure 9). Given the monomer functionality,  $f$ , and functional group stoichiometric ratio,  $r$ , the gel-point conversion is determined for a step-growth polymerization via the Flory-Stockmayer equation,  $p_{gel} = [r(f_a - 1)(f_b - 1)]^{-1/2}$ .<sup>96, 97</sup> Thus, the gel-point temperature is manipulated through monomer functionality, concentration, and stoichiometry as well as the thermodynamics and energetics of the specific thermoreversible coupling reaction. In contrast to the relatively simple reversion of low molecular weight, lower functionality systems that is readily shown, higher molecular weight linear polymers with pendant functional groups have a relatively low gel-point conversion, owing to their high functionality. These types of thermoreversible networks generally necessitate very high and generally impractical temperatures if they are to revert to an ungelled state.

While the thermodynamics predicts the gel-point temperature, the kinetics of the bond rearrangement dictates the characteristic mechanical properties of the network, specifically, the terminal relaxation. The forward reaction between the diene and dienophile is pseudo second order and the retro reaction is first order with respect to the adduct.<sup>12, 37, 94, 98</sup> Utilizing a kinetic model, the forward and reverse reaction rate constants of a network crosslink are determined from unsteady-state conversion versus time data.<sup>12</sup> The half-life of a crosslink, i.e., the adduct, is calculated from the reverse reaction rate constant,  $k_r$ , via  $t_{1/2} = \ln 2/k_r$ . For the system shown in Figure 8, this half-life is on the same order of magnitude as the inverse of the crossover frequency, confirming that the crossover in storage and loss moduli is owing to network rearrangement. By measuring  $k_r$  as a function of temperature, one finds that the



crosslink half-life increases from seconds to years, and the material behaves as a solid on most relevant timescales (graduate student and post-doc half-lives!).<sup>12</sup>

## 4. Applications of CANs

### 4.1. Thermoreversible Covalent Networks

The applications of CANs are those that require the mechanical properties of a covalent network, but simultaneously benefit from a lack of permanence in the structure as would be typical of a conventional thermoset. An associated potential disadvantage of these materials that must be considered is their long-term creep behavior that, depending on the specific chemical nature of the CAN, may lead to long-term changes in the material shape, particularly for those materials held under stress during their implementation. The creation of an easily recyclable material that possesses the characteristics of a thermoset has been a motivating idea since the inception of thermally controlled CANs<sup>20</sup> and a number of systems have been synthesized that are readily manipulated post-polymerization.<sup>12, 19, 20, 33, 39</sup> Thermal CANs have also been employed in so-called hot-melt applications, such as hot-melt inks<sup>99</sup> and hot-melt adhesives,<sup>6, 94</sup> where the material is manipulated in a heated liquid-state and then cooled to produce a crosslinked solid.

Electronic components are often protected from the environment in a thermoset encapsulate. If the component is found to be faulty after encapsulation, rework of the circuit requires shearing off the component and the thermoset encapsulate. Accordingly, the use of thermoreversible materials that can be easily removed has been explored as alternative encapsulates<sup>3-6</sup> and anisotropic conductive adhesives. Interestingly, in such applications the reverse reaction can be driven far from equilibrium by flushing sol fraction away with solvent. As a consequence, it is no longer necessary to drive the material past the conversion required for reverse gelation, rather only a sufficient rate of the reverse reaction is required. This strategy enables the use of polymers that are highly functionalized with crosslinking groups.

Thermoreversible crosslinks have been used to align dendritic non-linear optical chromophores to achieve high electrical optical coefficients.<sup>7, 8</sup> Crosslinking of the dendrimers reduces the free volume, improving the long term stability of the material. Furthermore, the reversible nature of the Diels-Alder reaction permits the materials to be cured until alignment is achieved. It is also possible to incorporate a second chromophore, without inducing phase separation that improves the poling efficiency.<sup>101</sup> Thermoreversible materials have also been employed as the cladding material in light guides and other electro-optic devices.<sup>102</sup>

More recent work has been directed at the use of thermoreversible bonds for creating self-healing materials.<sup>33, 42, 44, 45, 103</sup> Self-healing materials possess the ability to recover their initial mechanical properties after damage. On small size scales healing is nearly universal in polymers due to reptation of polymer chains though this behavior is limited in crosslinked polymer networks;<sup>104</sup> however, macroscopic crack healing is always a significantly more difficult challenge. Autonomic self-healing schemes, where monomer is encapsulated in spheres, fibers, or channels and is released upon fracture to flow and subsequently polymerize in the crack, have been shown to be successful, but suffer from a limited number of healing cycles as the monomer is depleted.<sup>105</sup> While polymers incorporating reversible bonds do not permit macroscale autonomous healing, they do offer a more simple approach to healing. For cracks where two surfaces are in close contact, bond rearrangement alone permits material healing. Chen et al.<sup>44, 45</sup> synthesized multifunctional furan and maleimide monomers and demonstrated, for a material above its gel point, 50% fracture toughness recovery after initial fracturing and 41% after a second fracture.<sup>44</sup> Second generation materials by the same group recovered 80% and 78% of their initial fracture toughness after two subsequent sample fracture and healing cycles.<sup>45</sup> Since reverse gelation in thermal CANs results in material flow, full

mechanical strength recovery is possible provided that irreversible side reactions, particularly common at elevated temperatures, are suppressed. Unfortunately, reverse gelation also results in slump or deformation in the overall material shape; thus, for many structural applications, near gel reversion is desirable.

#### 4.2. Photoreversible Covalent Networks

In one particular application of photoreversible CANs, photodimerization and photocleavage have been exploited to alter the mechanical properties of hydrogels reversibly.<sup>51, 60</sup> Hydrogels are commonly used as encapsulating and substrate media for cells<sup>106, 107</sup> thus many experiments utilizing adaptable networks to examine the effect of dynamic variation of mechanical properties on the local cell environment can be envisaged where the intimate and reversible control of the network structure enables studies not possible with other covalent or physical network structures. Although the irradiation wavelengths typically used for the dimerization and scission reactions extend well into the ultraviolet and are incompatible with cell viability, sensitization of both forward<sup>108-111</sup> and reverse<sup>112-114</sup> reactions using visible-light absorbing, radical generating compounds would be a facile path to cell-compatibility.

Applications for network rearrangement *via* photodimerization and photocleavage are not limited to complete network reverse gelation. Lendlein *et al.* utilized the reversible photodimerization of cinnamates to great effect in their implementation of photoinduced shape memory in permanently crosslinked polymers.<sup>56, 57</sup> Here, permanently crosslinked, elastomeric, (meth)acrylate polymers incorporating cinnamate functionalities were fabricated, strained and subject to irradiation at  $\lambda > 260$  nm. The incorporated cinnamate functionalities were dimerized during this irradiation step, increasing the crosslink density, and fixing the material into a new shape. Subsequent cleavage of the dimers by irradiation at  $\lambda < 260$  nm resulted in nearly complete recovery of the original shape of the material.

Another recently investigated application for photodimerization is light-induced crack healing. Chung *et al.*<sup>115</sup> found that the cyclobutane crosslinks in a material incorporating dimerized cinnamate groups were cleaved when the material was cracked, yielding the original, undimerized cinnamate groups. Subsequent heating, necessary to increase molecular mobility and allow for intimate contact between the two fracture surfaces, accompanied by concurrent irradiation of the cracked samples led to re-photodimerization of the surface cinnamate groups and a partial recovery of the flexural strength (see Figure 10).<sup>115</sup>

The combination of polymerization and adaptation is of particular relevance for applications where crosslinked networks are polymerized *in situ*, as shrinkage stress generally has a deleterious effect on the interface between the polymer network and the substrate and potentially on the substrate itself.<sup>116-118</sup> Recently, we utilized addition-fragmentation chain transfer concurrently with the polymerization reactions allowing network adaptivity via bond shuffling and reducing the polymerization shrinkage stress.<sup>78</sup> Monomers incorporating the allyl sulfide functionality were employed in a radical mediated, step-growth thiol-ene polymerization. To demonstrate conclusively that the polymerization stress reduction resulted from the addition-fragmentation reaction, analogous, nearly identical monomers (see Figure 11, panel A) and networks were formed: one containing allyl sulfide and a second containing propyl sulfide functionalities. The propyl sulfide-containing networks are essentially identical structurally although the elimination of the allyl sulfide renders them incapable of addition-fragmentation chain transfer. Upon polymerization, the shrinkage stress was >75% lower in the allyl sulfide-containing network as compared to the shrinkage stress developed in the propyl sulfide-containing network due to the addition-fragmentation chain transfer reaction leading to adaptation of the polymer network. This reduction in shrinkage stress in the allyl sulfide-containing networks was particularly apparent towards the end of the polymerization (see

Figure 11, panel B) where even the qualitative behavior is different with the allyl sulfide CAN exhibiting stress reduction and the propyl sulfide exhibiting a continued stress increase.<sup>78</sup>

## 5. Summary and Outlook

The utilization of reversible covalent chemistry in polymer networks yields a novel class of materials possessing network adaptability and yielding properties such as recyclability, healability, tunability, and low polymerization stress. Each of these attributes is complementary to the trend of polymeric materials becoming more tuned to specific applications. Ultimately, CANs constitute an emerging thrust for rational fabrication of smart materials capable of adapting to a predetermined stimulus.

Although much progress has been made in developing fabrication methodologies for novel thermo- and photo-reversible CANs, there still remains significant room for improvement, specifically in the continued incorporation of novel thermo- and photo-reversible moieties into covalent networks. Ideally, thermoreversible covalent linkages would revert at a specific application-relevant temperature, have rapid reaction kinetics, and low susceptibility to side reactions. New photoreversible linkages would target application relevant wavelengths, have enhanced photo-cleavage efficiencies, and low susceptibility to irreversible chain transfer and termination. Moreover, rational design of CANs requires an expansion in the characterization of mechanical properties, thermodynamics, and polymerization and reversion kinetics of these materials. As demonstrated above for the case of the trisfuran with bismaleimide, each of these areas are inherently related; however, this finding needs to be further explored in combination with theoretical developments.

## Acknowledgments

The authors acknowledge funding from the National Institutes of Health, NIH grant DE10959, the National Science Foundation Grant CBET 0626023 and 0933828, Department of Education GAANN Fellowship, and Sandia National Labs.

## Biographies



**Dr. Christopher J. Kloxin** received his B.S. in Chemical Engineering from the University of Colorado in 1999. He briefly worked at Eastman Kodak Company in Rochester, New York, after which he received his Ph.D. in Chemical Engineering from North Carolina State University in 2006. Currently, he is a research associate in chemical and biological engineering at the University of Colorado where his main research focus is on the implementation of reversible covalent linkages into covalent adaptable networks and their subsequent characterization.



**Professor Timothy F. Scott** received his B.S. (Hons) degree in Chemistry (2002) from the University of Melbourne and Ph.D. degree in Materials Engineering (2006) from Monash University. He then joined Prof. Bowman's group at the University of Colorado at Boulder where his research focused on radical-mediated polymerization and post-synthetic polymer manipulation. In 2008, he joined the Faculty of Mechanical Engineering at the University of Colorado at Boulder as a Research Assistant Professor, where he currently examines functional polymeric biomaterials and membranes.



**Brian J. Adzima** received his B.S. in Chemical Engineering from the University of Pittsburgh in 2005. He is currently a graduate student in Chemical Engineering at the University of Colorado, studying under the direction of Christopher N. Bowman. His research focuses on the synthesis, characterization, and application of thermal covalent adaptable networks.



**Professor Christopher N. Bowman** received his B.S. and Ph.D. in Chemical Engineering from Purdue University in 1988 and 1991, respectively. After receiving his Ph.D., he began his academic career at the University of Colorado in January of 1992 as an Assistant Professor. Since that time Professor Bowman has built a program focused on the fundamentals and applications of crosslinked polymers formed via photopolymerization reactions. He works in the broad areas of the fundamentals of polymerization reaction engineering, polymer chemistry, crosslinked polymers, photopolymerizations, and biomaterials. Professor Bowman has remained at Colorado throughout his academic career and is currently the Patten Endowed Chair of the Department of Chemical and Biological Engineering as well as a Clinical Professor of Restorative Dentistry at the University of Colorado at Denver. He serves as co-Director of the NSF/Industry Cooperative Research Center for Fundamentals and Applications of Photopolymerizations.

## References Cited

1. Grosberg, AY.; Khokhlov, AR. *Giant Molecules: Here, There, and Everywhere*. Academic Press; San Diego: 1997.
2. Flory, PJ. *Principles of Polymer Chemistry*. Cornell University Press; Ithaca, NY: 1953.
3. Iyer, SR.; Wong, PK. Thermally reworkable binders for flip chip devices. Jun 2. 1998 US Patent 5,760,337
4. Iyer, S.; Wong, PK. Die attach adhesive compositions. Oct 26. 1999 US Patent 5,973,052
5. Iyer, SR.; Wong, PK. Die attach adhesive compositions. Jun 15. 1999 US Patent 5,912,282
6. Small, JH.; Loy, DA.; McElhanon, JR.; Saunders, RS. Method of making thermally removable polymeric encapsulants. Aug 7. 2001 US Patent 6,271,335
7. Shi Z, Hau S, Luo J, Kim TD, Tucker NM, Ka JW, Sun H, Pyajt A, Dalton L, Chen A, Jen AKY. *Adv. Funct. Mater* 2007;17(14):2557–2563.
8. Enami Y, Derose CT, Mathine D, Loychik C, Greenlee C, Norwood RA, Kim TD, Luo J, Tian Y, Jen AKY, Peyghambarian N. *Nat. Photonics* 2007;1(3):180–185.
9. de Gennes, P-G. *Scaling concepts in polymer physics*. Cornell University Press; Ithaca: 1979.
10. Skene WG, Lehn JMP. *Proc. Natl. Acad. Sci. U. S. A* 2004;101(22):8270–8275. [PubMed: 15150411]

11. Rowan SJ, Cantrill SJ, Cousins GRL, Sanders JKM, Stoddart JF. *Angew. Chem.-Int. Edit* 2002;41(6):898–952.
12. Adzima BJ, Aguirre HA, Kloxin CJ, Scott TF, Bowman CN. *Macromolecules* 2008;41(23):9112–9117.
13. Heath WH, Palmieri F, Adams JR, Long BK, Chute J, Holcombe TW, Zieren S, Truitt MJ, White JL, Willson CG. *Macromolecules* 2008;41(3):719–726.
14. Long BK, Keitz BK, Willson CG. *J. Mater. Chem* 2007;17(34):3575–3580.
15. Hoyle CE, Lowe AB. *Chem. Soc. Rev.* 2009 In Press.
16. Engle LP, Wagener KB. *J. Macromol. Sci. - Rev. Macromol. Chem. Phys* 1993;C33(3):239–257.
17. Chang JY, Do SK, Han MJ. *Polymer* 2001;42(18):7589–7594.
18. Kamplain JW, Bielawski CW. *Chem. Commun* 2006;(16):1727–1729.
19. Higaki Y, Otsuka H, Takahara A. *Macromolecules* 2006;39(6):2121–2125.
20. Craven, JM. Cross-linked Thermally Reversible Polymers Produced from Condensation Polymers with Pendant Furan Groups Cross-linked with Maleimides. Mar 25. 1969 US Patent 3,435,003
21. Reutenauer P, Boul PJ, Lehn JM. *Eur. J. Org. Chem* 2009;(11):1691–1697.
22. Boul PJ, Reutenauer P, Lehn JM. *Org. Lett* 2005;7(1):15–18. [PubMed: 15624966]
23. van der Mee MAJ, Goossens JGP, van Duin M. *Polymer* 2008;49(5):1239–1248.
24. Amamoto Y, Higaki Y, Matsuda Y, Otsuka H, Takahara A. *J. Am. Chem. Soc* 2007;129(43):13298–13304. [PubMed: 17910457]
25. Wagener KB, Engle LP. *Macromolecules* 1991;24(26):6809–6815.
26. van der Mee MAJ, Goossens JGP, van Duin M. *J. Polym. Sci. Pol. Chem* 2008;46(5):1810–1825.
27. Amamoto Y, Kikuchi M, Masunaga H, Sasaki S, Otsuka H, Takahara A. *Macromolecules* 2009;42(22):8733–8738.
28. Danen WC, Newkirk DD. *J. Am. Chem. Soc* 1976;98(2):516–520.
29. Maillard B, Ingold KU. *J. Am. Chem. Soc* 1976;98(2):520–523.
30. Kolb HC, Finn MG, Sharpless KB. *Angew. Chem.-Int. Edit* 2001;40(11):2004–2021.
31. Fringuelli, F.; Taticchi, A. *The Diels-Alder reaction: selected practical methods.* John Wiley & Sons, Inc.; New York: 2002.
32. Kennedy JP, Castner KF. *J. Polym. Sci. Pol. Chem* 1979;17(7):2055–2070.
33. Murphy EB, Bolanos E, Schaffner-Hamann C, Wudl F, Nutt SR, Auad ML. *Macromolecules* 2008;41(14):5203–5209.
34. Laita H, Boufi S, Gandini A. *Eur. Polym. J* 1997;33(8):1203–1211.
35. Gousse C, Gandini A, Hodge P. *Macromolecules* 1998;31(2):314–321.
36. Gheneim R, Perez-Berumen C, Gandini A. *Macromolecules* 2002;35(19):7246–7253.
37. Goiti E, Heatley F, Huglin MB, Rego JM. *Eur. Polym. J* 2004;40(7):1451–1460.
38. Goiti E, Huglin MB, Rego JM. *Eur. Polym. J* 2004;40(2):219–226.
39. Liu YL, Hsieh CY. *J. Polym. Sci. Pol. Chem* 2006;44(2):905–913.
40. Liu YL, Chen YW. *Macromol. Chem. Phys* 2007;208(2):224–232.
41. Kavitha AA, Singha NK. *Macromol. Chem. Phys* 2007;208(23):2569–2577.
42. Zhang Y, Broekhuis AA, Picchioni F. *Macromolecules* 2009;42(6):1906–1912.
43. Imai Y, Itoh H, Naka K, Chujo Y. *Macromolecules* 2000;33(12):4343–4346.
44. Chen XX, Dam MA, Ono K, Mal A, Shen HB, Nutt SR, Sheran K, Wudl F. *Science* 2002;295(5560):1698–1702. [PubMed: 11872836]
45. Chen XX, Wudl F, Mal AK, Shen HB, Nutt SR. *Macromolecules* 2003;36(6):1802–1807.
46. Watanabe M, Yoshie N. *Polymer* 2006;47(14):4946–4952.
47. Gotsmann B, Duerig U, Frommer J, Hawker CJ. *Adv. Funct. Mater* 2006;16(11):1499–1505.
48. Ishida K, Yoshie N. *Macromol. Biosci* 2008;8(10):916–922. [PubMed: 18551456]
49. Liu YL, Hsieh CY, Chen YW. *Polymer* 2006;47(8):2581–2586.
50. Reutenauer P, Buhler E, Boul PJ, Candau SJ, Lehn JM. *Chem.-Eur. J* 2009;15(8):1893–1900.
51. Nagata M, Yamamoto Y. *React. Funct. Polym* 2008;68(5):915–921.

52. Nagata M, Yamamoto Y. *J. Polym. Sci. Pol. Chem* 2009;47(9):2422–2433.
53. Zhao DL, Ren BY, Liu SS, Liu XX, Tong Z. *Chem. Commun* 2006;(7):779–781.
54. Ren BY, Zhao DL, Liu SS, Liu XX, Tong Z. *Macromolecules* 2007;40(13):4501–4508.
55. Trenor SR, Shultz AR, Love BJ, Long TE. *Chem. Rev* 2004;104(6):3059–3077. [PubMed: 15186188]
56. Lendlein A, Jiang HY, Junger O, Langer R. *Nature* 2005;434(7035):879–882. [PubMed: 15829960]
57. Jiang HY, Kelch S, Lendlein A. *Adv. Mater* 2006;18(11):1471–1475.
58. Zheng YJ, Andreopoulos FM, Micic M, Huo Q, Pham SM, Leblanc RM. *Adv. Funct. Mater* 2001;11(1):37–40.
59. Micic M, Zheng YJ, Moy V, Zhang XH, Andreopoulos FM, Leblanc RM. *Colloid Surf. B-Biointerfaces* 2003;27(23):147–158.
60. Gattas-Asfura KM, Weisman E, Andreopoulos FM, Micic M, Muller B, Sirpal S, Pham SM, Leblanc RM. *Biomacromolecules* 2005;6(3):1503–1509. [PubMed: 15877371]
61. Zheng YJ, Micie M, Mello SV, Mabrouki M, Andreopoulos FM, Konka V, Pham SM, Leblanc RM. *Macromolecules* 2002;35(13):5228–5234.
62. Connal LA, Vestberg R, Hawker CJ, Qiao GG. *Adv. Funct. Mater* 2008;18(20):3315–3322.
63. Matsui J, Ochi Y, Tamaki K. *Chem. Lett* 2006;35(1):80–81.
64. Imai Y, Ogoshi T, Naka K, Chujo Y. *Polym. Bull* 2000;45(1):9–16.
65. Hall DN, Oswald AA, Griesbau K. *J. Org. Chem* 1965;30(11):3829–3834.
66. Hall DN. *J. Org. Chem* 1967;32(7):2082–2087.
67. Meijs GF, Rizzardo E, Thang SH. *Macromolecules* 1988;21(10):3122–3124.
68. Meijs GF, Morton TC, Rizzardo E, Thang SH. *Macromolecules* 1991;24(12):3689–3695.
69. Evans RA, Moad G, Rizzardo E, Thang SH. *Macromolecules* 1994;27(26):7935–7937.
70. Evans RA, Rizzardo E. *Macromolecules* 1996;29(22):6983–6989.
71. Evans RA, Rizzardo E. *Macromolecules* 2000;33(18):6722–6731.
72. Harrisson S, Davis TP, Evans RA, Rizzardo E. *Macromolecules* 2000;33(26):9553–9560.
73. Evans RA, Rizzardo E. *J. Polym. Sci. Pol. Chem* 2001;39(1):202–215.
74. Harrisson S, Davis TP, Evans RA, Rizzardo E. *Macromolecules* 2001;34(12):3869–3876.
75. Harrisson S, Davis TP, Evans RA, Rizzardo E. *Macromolecules* 2002;35(7):2474–2480.
76. Scott TF, Schneider AD, Cook WD, Bowman CN. *Science* 2005;308(5728):1615–1617. [PubMed: 15947185]
77. Scott TF, Draughon RB, Bowman CN. *Adv. Mater* 2006;18(16):2128–2132.
78. Kloxin CJ, Scott TF, Bowman CN. *Macromolecules* 2009;42(7):2551–2556. [PubMed: 20160931]
79. Tobolsky AV, Prettyman IB, Dillon JH. *J. Appl. Phys* 1944;15(4):380–395.
80. Andrews RD, Tobolsky AV, Hanson EE. *J. Appl. Phys* 1946;17(5):352–361.
81. Ermoshkin AA, Neckers DC, Fedorov AV. *Macromolecules* 2006;39(17):5669–5674.
82. Ermoshkin AA, Nikolaeva ES, Neckers DC, Fedorov AV. *Macromolecules* 2008;41(23):9063–9066.
83. Bowman CN, Kloxin CJ. *AIChE J* 2008;54(11):2775–2795.
84. Nijenhuis KT. Thermoreversible networks - Viscoelastic properties and structure of gels - Introduction. *Thermoreversible Networks* 1997;130:1–12.
85. Winter HH, Chambon F. *J. Rheol* 1986;30(2):367–382.
86. Winter HH. *Polym. Eng. Sci* 1987;27(22):1698–1702.
87. Chambon F, Winter HH. *J. Rheol* 1987;31(8):683–697.
88. Chambon F, Winter HH. *Polym. Bull* 1985;13(6):499–503.
89. Hess W, Vilgis TA, Winter HH. *Macromolecules* 1988;21(8):2536–2542.
90. Muthukumar M. *Macromolecules* 1989;22(12):4656–4658.
91. Derosa ME, Winter HH. *Rheol. Acta* 1994;33(3):220–237.
92. Tanaka F, Edwards SF. *J. Non-Newton. Fluid Mech* 1992;43(23):273–288.
93. McElhanon JR, Russick EM, Wheeler DR, Loy DA, Aubert JH. *J. Appl. Polym. Sci* 2002;85(7):1496–1502.
94. Tian Q, Yuan YC, Rong MZ, Zhang MQ. *J. Mater. Chem* 2009;19(9):1289–1296.

95. Ishida K, Yoshie N. *Macromolecules* 2008;41(13):4753–4757.
96. Flory PJ. *J. Am. Chem. Soc* 1941;63(11):3083–3090.
97. Stockmayer WH. *J. Chem. Phys* 1943;11(2):45–55.
98. Goiti E, Huglin MB, Rego JM. *Macromol. Rapid Commun* 2003;24(11):692–696.
99. Paine AJ, Hamer GK, Tripp CP, Bareman JP, Mayer FM, Sacripante GG. Phase change ink compositions. December 1;1998 5,844,020.
100. Iyer, SR.; Wong, PK. Anisotropic conductive adhesives compositions. Nov 24. 1998 US Patent 5,840,215
101. Kim TD, Luo J, Ka JW, Hau S, Tian Y, Shi Z, Tucker NM, Jang SH, Kang JW, Jen AKY. *Adv. Mater* 2006;18(22):3038–3042.
102. Jen, K-Y.; Luo, J.; Liu, S. Thermally reversibly crosslinkable polymer as cladding for electro-optic devices. Mar 18. 2008 US Patent 7,346,259
103. Bergman SD, Wudl F. *J. Mater. Chem* 2008;18(1):41–62.
104. Wool RP. *Soft Matter* 2008;4(3):400–418.
105. White SR, Sottos NR, Geubelle PH, Moore JS, Kessler MR, Sriram SR, Brown EN, Viswanathan S. *Nature* 2001;409(6822):794–797. [PubMed: 11236987]
106. Bryant SJ, Chowdhury TT, Lee DA, Bader DL, Anseth KS. *Ann. Biomed. Eng* 2004;32(3):407–417. [PubMed: 15095815]
107. Ghosh K, Pan Z, Guan E, Ge SR, Liu YJ, Nakamura T, Ren XD, Rafailovich M, Clark RAF. *Biomaterials* 2007;28(4):671–679. [PubMed: 17049594]
108. Lamola AA, Yamane T. *Proc. Natl. Acad. Sci. U. S. A* 1967;58(2):443–446. [PubMed: 4292974]
109. Meistrich ML, Lamola AA. *J. Mol. Biol* 1972;66(1):83–95. [PubMed: 4557199]
110. Karthikeyan S, Ramamurthy V. *Tetrahedron Lett* 2005;46(26):4495–4498.
111. Islangulov RR, Castellano FN. *Angew. Chem.-Int. Edit* 2006;45(36):5957–5959.
112. Sasson S, Elad D. *J. Org. Chem* 1972;37(20):3164–&.
113. Hartman RF, Rose SD. *J. Am. Chem. Soc* 1992;114(9):3559–3560.
114. Tung CH, Ying YM, Yuan ZY. *J. Photochem. Photobiol. A-Chem* 1998;119(2):93–99.
115. Chung CM, Roh YS, Cho SY, Kim JG. *Chem. Mat* 2004;16(21):3982–3984.
116. Davidson CL, Feilzer AJ. *J. Dent* 1997;25(6):435–440. [PubMed: 9604575]
117. Labella R, Lambrechts P, Van Meerbeek B, Vanherle G. *Dent. Mater* 1999;15(2):128–137. [PubMed: 10551104]
118. Lu H, Carioscia JA, Stansbury JW, Bowman CN. *Dent. Mater* 2005;21(12):1129–1136. [PubMed: 16046231]



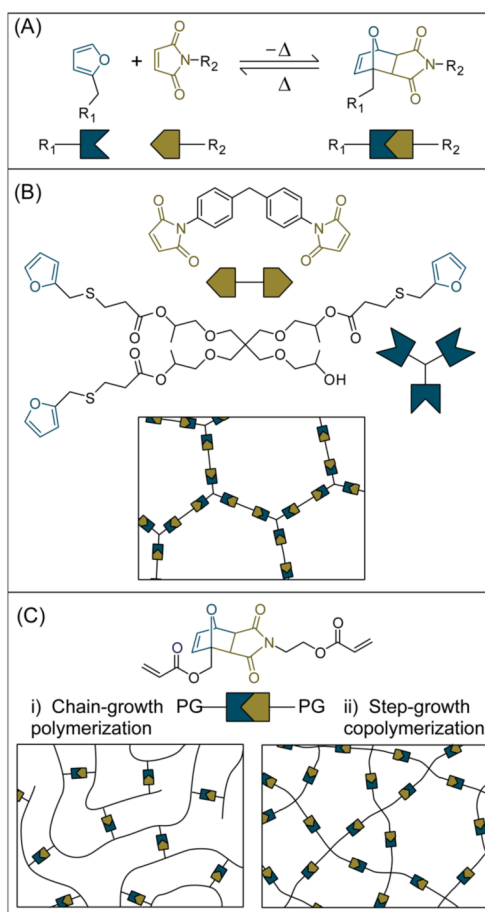


**Figure 1. The thermoreversible Diels-Alder (DA) reaction between furan and maleimide (panel A) is used to demonstrate CAN fabricated by formation of the reversible linkage (panel B) or by polymerizable functionality flanking the reversible linkage (panel C)**

In each of the panels, the reaction between maleimide and furan are represented as complementary geometric shapes. In panel A, the DA cycloaddition between furan (left) and maleimide (middle), which forms the bicyclic compound (right) at low temperatures, is shown. This model thermoreversible reaction undergoes the retro-Diels-Alder reaction at elevated temperatures. In panel B, the network is formed by bismaleimide and trisfuran monomers<sup>12</sup> that undergo a step-growth polymerization via the reversible linkage. In panel C, the reversible CAN linkage is flanked by two polymerizable groups (PG) which, as an example, are given as acrylate functional groups. These acrylate functional groups can be either *i*) polymerized via a radical-mediated chain-growth mechanism<sup>13, 14</sup> or *ii*) co-polymerized with a multifunctional thiol monomer (e.g., pentaerythritol-tetrakis-3-mercaptopropionate) via base-catalyzed Michael addition.<sup>15</sup> The insets of B and C represent the formed network structure, which contains reversible linkages that enable reversible depolymerization. It should be noted that although a thermoreversible CAN was used as an example, this demonstration of polymerization types is equally applicable for photoreversible CANs.

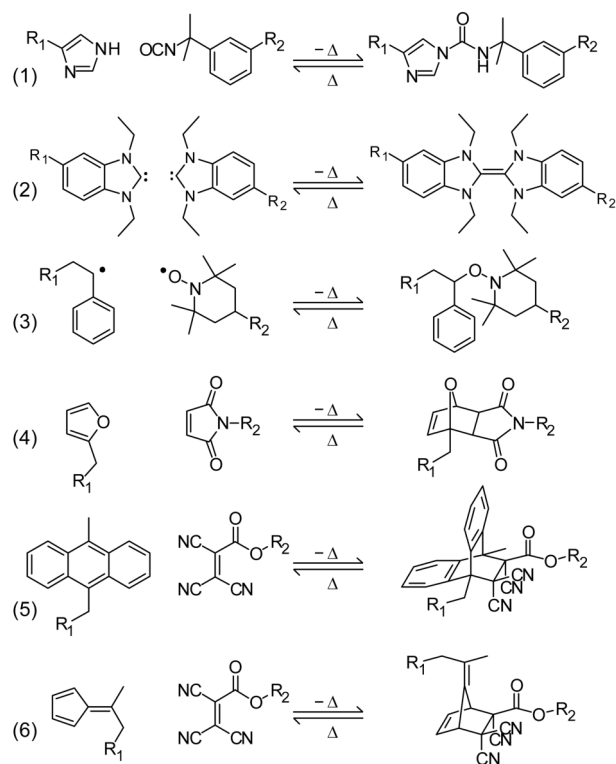


**Figure 2. A selection of thermoreversible crosslinking addition reactions**

Here, we show the thermoreversible 1) nucleophilic addition between isocyanate and imidazole,<sup>17</sup> 3) carbene dimerization,<sup>18</sup> 2) reversible radical coupling between TEMPO and a styryl radical,<sup>19</sup> and the DA cycloaddition between 4) furan and maleimide,<sup>20</sup> 5) anthracene and cyanoacrylate,<sup>21</sup> and 6) fulvene and cyanoacrylate<sup>22</sup> (only exo product is shown).

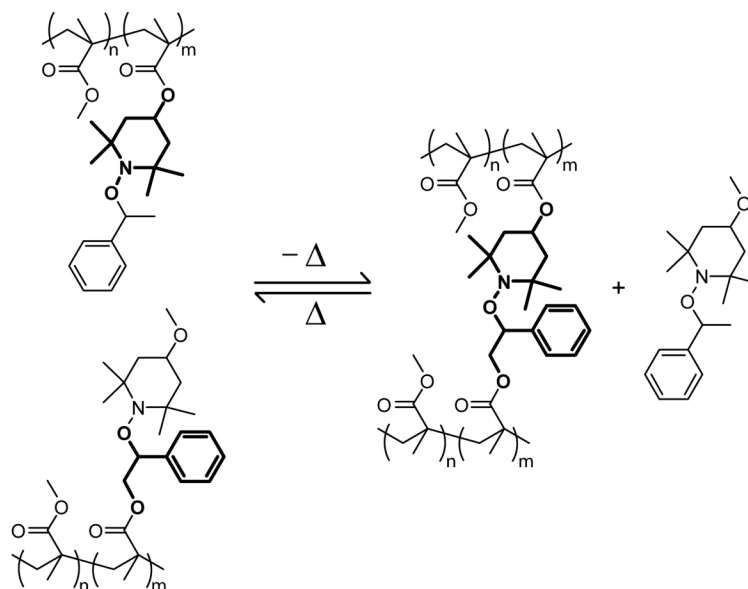


**Figure 3. Thermoreversible homolytic cleavage of alkoxyamine producing linear chains with pendant styryl and TEMPO radicals.<sup>19</sup>**

In this radical crossover reaction, heating causes the capping styryl and TEMPO functional groups to dissociate from their respective linear chain, revealing a pendant TEMPO radical from one chain and a pendant styryl radical from another chain that are capable of forming a thermoreversible crosslink. The small molecular styryl and TEMPO capping species are also able to thermoreversibly combine.

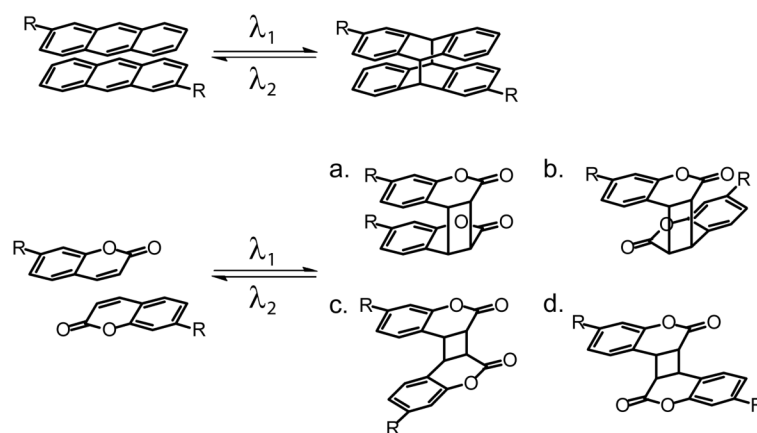


**Figure 4. Photodimerization of coumarin and anthracene as controlled by irradiation wavelength**  
The four potential isomers resulting from the [2+2] coumarin dimerization include a) head-to-head, syn; b) head-to-head, anti; c) head-to-tail, syn; and, d) head-to-tail, anti. For clarity, one of the four potential isomers resulting from the [4+4] anthracene dimerization is shown.

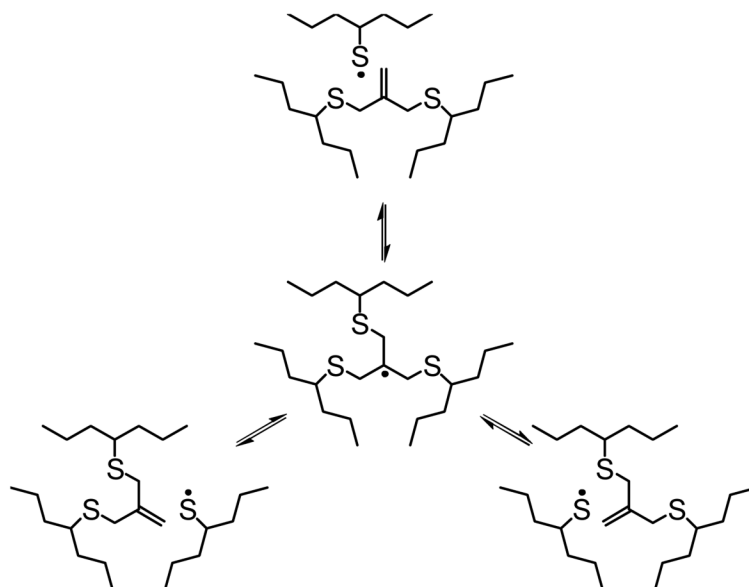


**Figure 5. Radical-mediated addition-fragmentation chain transfer allows for rearrangement of polymer connectivity**

The thiyl radical and the allyl sulfide units in the polymer are in a dynamic pseudoequilibrium relation where the thiyl radical catalyzes the cleavage and reformation of the allyl sulfide linkages in the polymer network.

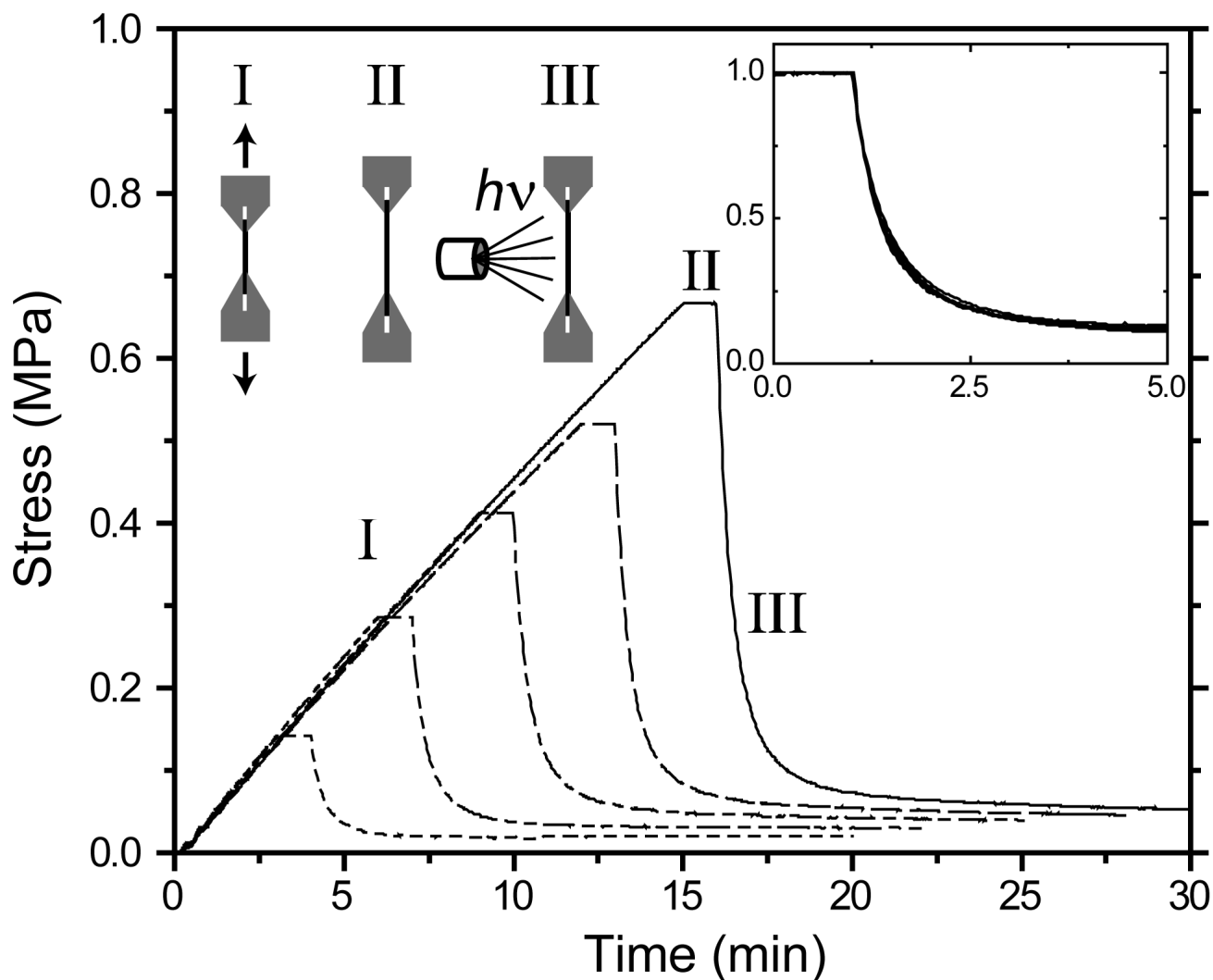


**Figure 6.** Photoinduced stress relaxation (i.e., permanent set) of an allyl sulfide thiol-ene network.  
76

The sample is (I) uniaxially stretched to 1.5 (dotted), 3.0 (dot-dot-dash), 4.5 (dot-dash), 6.0 (dash), and 7.5 % (solid) strain, (II) held at constant strain for 1 min, and (III) irradiated with 365 nm light at an intensity of 40 mW/cm<sup>2</sup>. The inset shows the time shifted (to the beginning of phase II) and normalized stress, which demonstrates 90% stress reduction for all the samples presented here. Adapted from reference <sup>83</sup>.

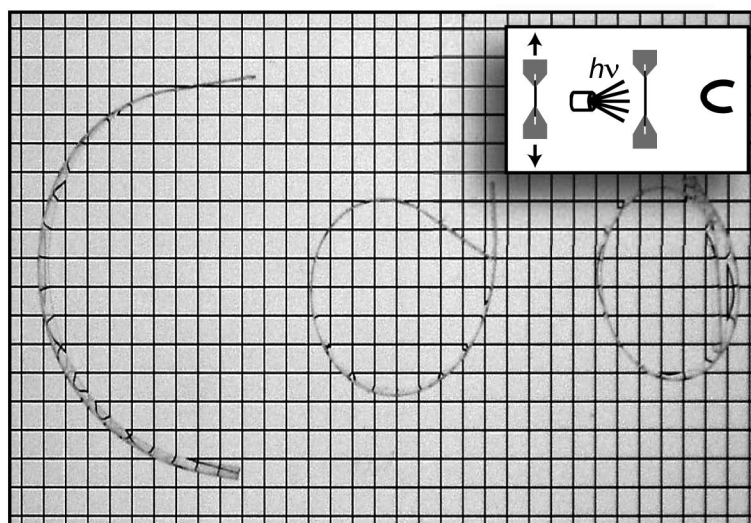


**Figure 7. Samples containing allyl sulfide deforming in response to stress gradient ‘written’ via light attenuation through the sample.<sup>77</sup>**

As shown in the inset, the samples are uniaxially stretched and irradiated (365 nm light at 40 mW/cm<sup>2</sup> for 30, 60, and 90s – left to right), triggering bond rearrangement via addition-fragmentation of allyl sulfide functional groups in the network backbone. Since the samples are optically thick (using ultraviolet light absorber), the light is attenuated, producing a gradient of active bond rearrangement and thus a gradient in stress. After irradiation, the samples deform by warping to equalize the internal stresses.

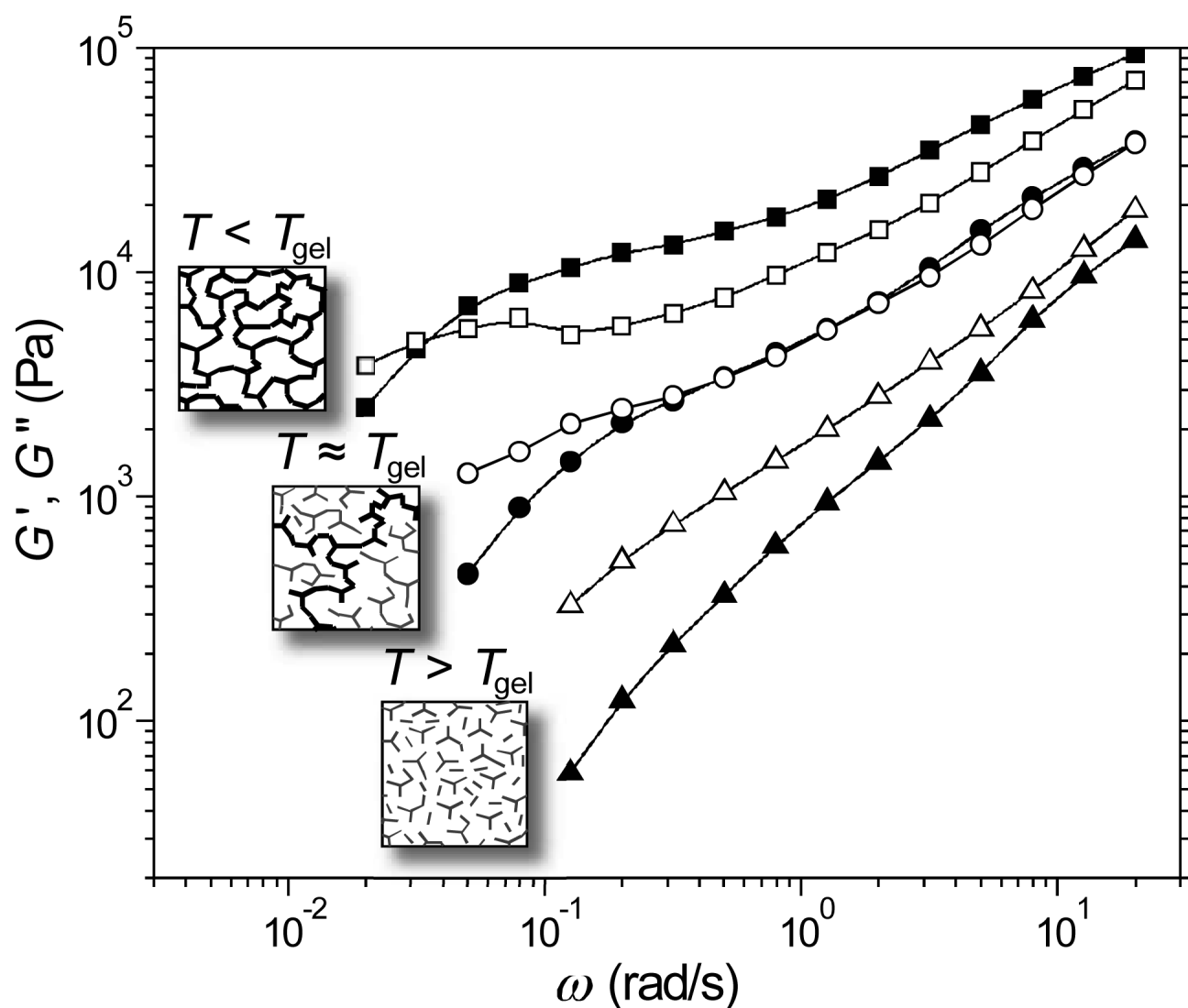
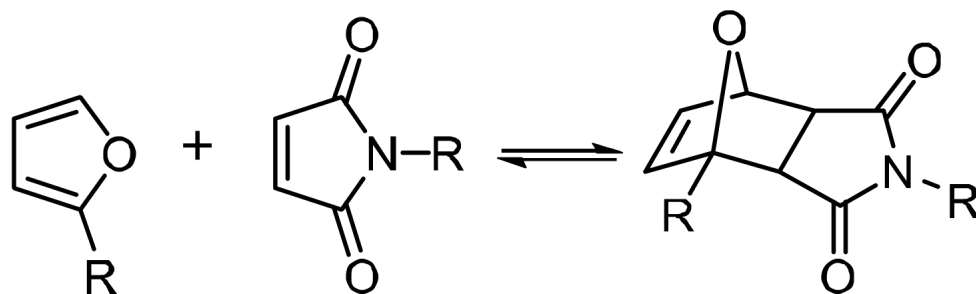


**Figure 8. Elastic (closed symbols) and viscous (open symbols) moduli as a function of angular frequency for a stoichiometric bismaleimide and trisfuran monomer mixture above (triangles, 95°C), near (circles, 91°C), and below (squares, 87°C) the gel-point temperature**  
 For all temperatures, the terminal behavior (i.e.,  $\omega \rightarrow 0$ ) approaches that of a viscoelastic liquid ( $G' \sim \omega^2$  and  $G'' \sim \omega^1$ ). The moduli exhibit similar frequency scaling ( $G' \sim G'' \sim \omega^{0.56}$ ) at the gel-point temperature, corresponding well to that determined by the Flory-Stockmayer gel-point conversion determined by FTIR ( $92.5 \pm 0.5^\circ\text{C}$ ). Adapted from reference <sup>12</sup>.





$$\ln K = \frac{-\Delta H_{rxn}}{RT} + \frac{\Delta S_{rxn}}{R}$$

$$K = \frac{rp_E}{c_0 (1 - p_E)(1 - rp_E)}$$



$$T_{gel} = \frac{\Delta H_{rxn}}{\Delta S_{rxn} - \ln \frac{rp_{E,gel}}{c_0 (1 - p_{E,gel})(1 - rp_{E,gel})}}$$

Figure 9. The relationship between the gel-point temperature,  $T_{gel}$ , and conversion,  $p_{E,gel}$ , for the reaction between diene and dienophile (shown as furan and maleimide functional groups, respectively, where R is the connectivity to the remainder of the monomer structure) is related through the initial functional group concentration,  $c_0$ , equilibrium conversion,  $p_E$ , heat of reaction,  $\Delta H_{rxn}$ , and entropy of reaction,  $\Delta S_{rxn}$

For the case that the diene and dienophile are not stoichiometric,  $r$  is the stoichiometric ratio defined as the limiting functional group concentration divided by the functional group concentration in excess, and where  $c_0$  and  $p_{E,gel}$  are the limiting functional group concentration and conversion, respectively.

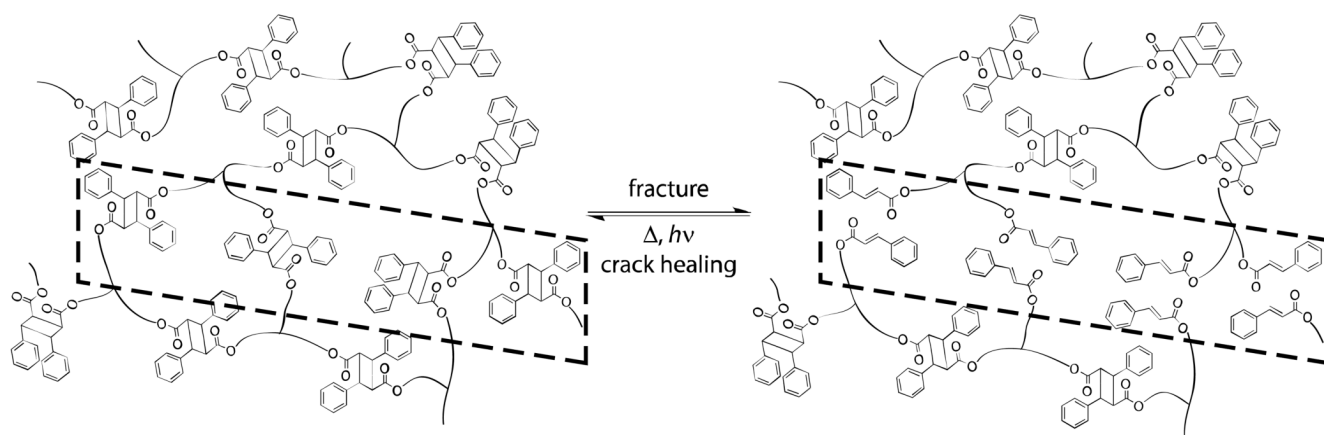


**Figure 10. Schematic of photoinduced cinnamate crack healing.**<sup>115</sup>

Crack propagation in a cinnamate crosslinked network promotes the retro-[2+2] cycloaddition as evidenced by the appearance of a C=C absorption monitored by infrared spectroscopy. The subsequent photo-induced healing of the crack resulted in an increase in flexural strength as well as a reduction of the C=C absorption. Adapted from reference <sup>115</sup>.

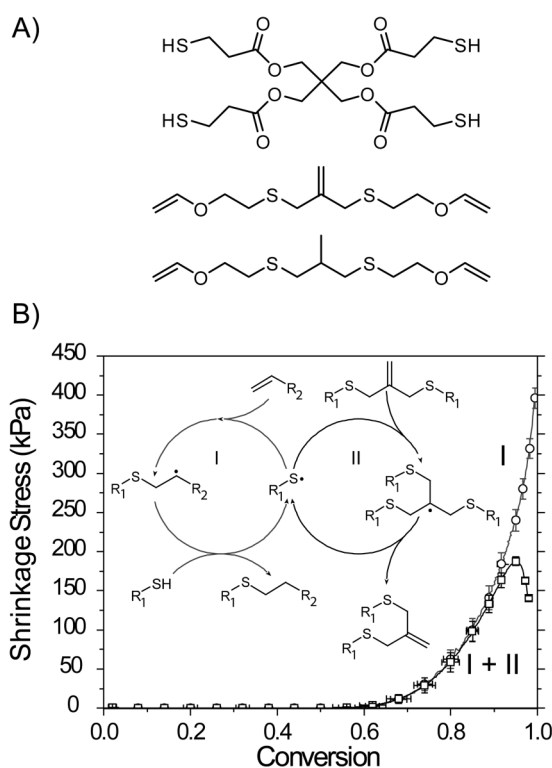


**Figure 11. Using a model thiol-ene photopolymerization of a tetra-thiol (panel A, top) and an allyl sulfide divinyl ether (panel A, middle), a reduction in polymerization stress (panel B) was achieved when compared to the analogue tetra-thiol and propyl sulfide divinyl ether (panel A, bottom) thiol-ene photopolymerization**

In panel B the polymerization stress is measured as a function of conversion, where the propyl sulfide-based material exhibits an increase in stress at the gel point (~58% conversion) that continues until achieving full conversion. The propyl sulfide monomer is incapable of undergoing addition-fragmentation and thus only follows the step growth mechanism shown as cycle I (inset). While the allyl sulfide-based material also exhibits an increase in stress at the gel point, the evolution in stress reaches a maximum followed by a decrease that is roughly  $1/3^{\text{rd}}$  the stress of analogue. The allyl sulfide monomer is capable of both the step-growth mechanism (cycle I, inset) as well as the addition-fragmentation mechanism (cycle II, inset), which is responsible for the observed decrease in stress. Adapted from reference <sup>78</sup>.